

Probing natural SUSY from stop pair production at the LHC

Junjie Cao^{1,2}, Chengcheng Han³, Lei Wu³, Jin Min Yang³, Yang Zhang^{1,3}

¹ *Physics Department, Henan Normal University, Xinxiang 453007, China*

² *Center for High Energy Physics, Peking University, Beijing 100871, China*

³ *Institute of Theoretical Physics, Academia Sinica, Beijing 100190, China*

Abstract

We consider the natural supersymmetry scenario in the framework of the R -parity conserving minimal supersymmetric standard model (called natural MSSM) and examine the observability of stop pair production at the LHC. We first scan the parameters of this scenario under various experimental constraints, including the SM-like Higgs boson mass, the indirect limits from precision electroweak data and B-decays. Then in the allowed parameter space we study the stop pair production at the LHC followed by the stop decay into a top quark plus a lightest neutralino or into a bottom quark plus a chargino. From detailed Monte Carlo simulations of the signals and backgrounds, we find the two decay modes are complementary to each other in probing the stop pair production, and the LHC with $\sqrt{s} = 14$ TeV and 100 fb^{-1} luminosity is capable of discovering the stop predicted in natural MSSM up to 450 GeV. If no excess events were observed at the LHC, the 95% C.L. exclusion limits of the stop masses can reach around 537 GeV.

PACS numbers: 14.80.Da, 14.80.Ly, 12.60.Jv

I. INTRODUCTION

Although the standard model (SM) has been successful in describing the existing experimental data, it is suffering from the hierarchy problem and new physics based on certain symmetry is widely expected to appear at TeV scale to stabilize the electroweak hierarchy against radiative corrections. This belief was further strengthened by the recent discovery of the Higgs boson at the Large Hadron Collider (LHC) with its mass determined around 125 GeV [1]. This mass value agrees well with the prediction of low energy supersymmetry (SUSY), which is so far the most promising new physics candidate.

In SUSY, all known bosons and fermions have their supersymmetric partners, and the scalar top quarks (called stop \tilde{t}_i with $i = 1, 2$), as the top quark partners, can modify the property of the SM Higgs boson by exactly canceling out the dangerous quadratic divergence of the top quark loop. Obviously, the experimental determination of the stop properties is crucial to unravel the nature of supersymmetry in protecting the Higgs mass at the weak scale and thus solving the hierarchy problem. In fact, such activities have been carried out extensively at the hadronic colliders such as the LHC and the Tevatron [2–4], but in contrast with the strong mass bounds (about 1 TeV) on the gluino and the first generation squarks [5], a relatively light stop (say about 300 GeV) can not be excluded. Nevertheless, it should be mentioned that the recently measured Higgs boson mass around 125 GeV may give some indications for the stop sector[6–8]. In the popular MSSM with moderate $\tan\beta$ and large m_A , the Higgs mass is given by [6]

$$m_h^2 \simeq M_Z^2 \cos^2 2\beta + \frac{3m_t^4}{4\pi^2 v^2} \ln \frac{M_S^2}{m_t^2} + \frac{3m_t^4}{4\pi^2 v^2} \frac{X_t^2}{M_S^2} \left(1 - \frac{X_t^2}{12M_S^2} \right), \quad (1)$$

where $v = 174$ GeV, $X_t \equiv A_t - \mu \cot\beta$ and M_S is the average stop mass scale defined by $M_S = \sqrt{m_{\tilde{t}_1} m_{\tilde{t}_2}}$. This expression indicates that, for the heavier stop \tilde{t}_2 around 1 TeV as discussed above, the lighter stop \tilde{t}_1 must be heavier than about 200 GeV and $|X_t|$ must be larger than 1.5 TeV in order to push the Higgs mass up to 125 GeV [8]. About these constraints, one should keep in mind that they are independent of the decay modes of \tilde{t}_1 , but on the other hand, they may be greatly weakened if there exists additional contribution to the Higgs mass [8, 9].

On the theoretical side, there are good reasons to consider at least one stop significantly lighter than other squarks with a mass around several hundred GeV. Firstly, in some popular grand unification models, supersymmetry breaking is usually assumed to transmit to

the visible sector at a certain high energy scale, and then Yukawa contributions to the renormalization group evolution tend to reduce stop masses more than other squark masses. Secondly, the chiral mixing for certain flavor squarks is proportional to the mass of the corresponding quark, and is therefore more sizable for stops. Such a mixing will further reduce the mass of the lighter stop. Thirdly, in the MSSM the minimization conditions of its Higgs potential imply [10]

$$\frac{M_Z^2}{2} = \frac{(m_{H_d}^2 + \Sigma_d) - (m_{H_u}^2 + \Sigma_u) \tan^2 \beta}{\tan^2 \beta - 1} - \mu^2, \quad (2)$$

where $m_{H_d}^2$ and $m_{H_u}^2$ represent the weak scale soft SUSY breaking masses of the Higgs fields, μ is the higgsino mass parameter, $\tan \beta \equiv v_u/v_d$. Σ_u and Σ_d arise from the radiative corrections to the Higgs potential and the dominant contribution to the Σ_u is given by

$$\Sigma_u \sim \frac{3Y_t^2}{16\pi^2} \times m_{\tilde{t}_i}^2 \left(\log \frac{m_{\tilde{t}_i}^2}{Q^2} - 1 \right). \quad (3)$$

These two equations indicate that, if the individual terms on the right hand side of Eq. (2) are comparable in magnitude so that the observed value of M_Z is obtained without resorting to large cancelations, the natural values of μ and $m_{\tilde{t}_i}$ should be around 100 GeV and several hundred GeV respectively. Numerically, the requirement of $\Sigma_u < M_Z^2/2$ (or $\Sigma_u < v^2$) leads to $m_{\tilde{t}_{1,2}}$ upper bounded by about 500 GeV (or 1.5 TeV) [11]. Moreover, we note that a light stop is also phenomenologically needed by the electroweak baryogenesis [12] and may be welcomed by the dark matter physics [13]. In the MSSM, although the gluino contribute to $m_{\tilde{t}_i}^2$ at the one-loop level and to $m_{H_u}^2$ at two-loop level, the corrections are proportional to $m_{\tilde{g}}^2$ and can be greatly enhanced by the large gluino mass[14]. In order to keep the naturalness, we expect $m_{\tilde{g}}$ to be lighter than about 3 TeV for $m_{\tilde{t}} < 1.5$ TeV. However, since the current results of searching for the supersymmetry indicate that a gluino with mass about 1 TeV can safely avoid the LHC constraints, we require $1 \text{ TeV} < m_{\tilde{g}} < 3 \text{ TeV}$ in our calculation.

Motivated by the theoretical preference and the results of the LHC search for SUSY, recently the natural MSSM scenario attracted broad attention [14–18], which focuses on the following parameter space of the MSSM [14, 17]:

- $|\mu| \lesssim 100 - 200 \text{ GeV}$ and $m_{\tilde{t}_{1,2}} \leq 1 - 1.5 \text{ TeV}$ as preferred by Eq.(2) and Eq.(3);

- $1 \text{ TeV} \lesssim m_{\tilde{g}} \lesssim 3\text{-}4 \text{ TeV}$ to escape the LHC constraint and at same time to avoid spoiling color symmetry; while the electroweak-ino masses may still be at sub-TeV scale;
- $m_A \sim |m_{H_d}^2|^{\frac{1}{2}} \lesssim |\mu| \tan \beta$ as suggested by the relation $m_A^2 \simeq 2\mu^2 + m_{H_u}^2 + m_{H_d}^2 + \Sigma_u + \Sigma_d$ and Eq.(2);
- $m_{\tilde{q}_{1,2}}, m_{\tilde{l}_{1,2}} \sim 10 - 50 \text{ TeV}$ to provide a decoupling solution to the SUSY flavor and CP problems.

Since the stop are relatively light and sensitive to probing this scenario, there have been recently many theoretical studies on the collider signatures of the light directly produced stop in the R -parity conserving and violating MSSM[19]. For example, by using the top tagging technique, the sensitivity of stop searches were studied in the hadronic, semi-leptonic and di-leptonic channels[20–23]. In order to suppress the di-leptonic top backgrounds, the authors in Ref.[24] explore some new kinematic observables developed from M_{T_2} to improve the sensitivity of the stop searches. For the small mass splitting between stop and top, it is pointed that the rapidity difference and spin correlation of the daughter products from stops decay can be helpful to discover the signal[25]. When the stop mass is close to the lightest supersymmetric particle mass, the monojet signature from $\tilde{t}_1 \tilde{t}_1^* + j$ production is expected to be useful in detecting the stop[26]. If the stop mass is degenerate with the sum of the masses of its decay products, the searches based on missing transverse energy (E_T^{miss} or \cancel{E}_T) have significant reach for stop masses above 175 GeV[27]. When the R -parity is violated, the decay modes of the stop will be very different from the ones in R -parity conserving MSSM, such as stop decaying to dilepton and trilepton final states[28]. We also noted that the constrains on the light stop in the natural SUSY have been discussed by using the results from sparticles searches at the LHC, and indicated that they were mild and can be safely avoided currently[14, 17, 18, 29].

In this work, we investigate the potential of the LHC in probing the lighter stop \tilde{t}_1 predicted by the natural MSSM with R -parity, which is based on some considerations: (i) Most of the studies of the stop searches have been carried out under some assumptions at the LHC in a model independent way or in simplified models. It will be meaningful to explore what might happen in a realistic model like MSSM under the current available experimental constraints; (ii) Due to the R -parity conservation, there will be sizeable missing

energy appearing in the sparticles productions and decays, which can be easily identified in the LHC data; (iii) One interesting phenomenological feature of the natural MSSM with R -parity is that both the lightest neutralino and the lighter chargino are Higgsino-like, and consequently \tilde{t}_1 always decays dominantly into $t\tilde{\chi}_1^0$ and $b\tilde{\chi}_1^+$ with $\tilde{\chi}_1^+ \rightarrow \tilde{\chi}_1^0 W^*$, which can greatly simplify the analysis of the \tilde{t}_1 detection at the LHC.

For this purpose, we first scan the parameter space of the natural MSSM by considering various constraints in Sec. II. Then in Sec. III we discuss the observability of \tilde{t}_1 through the direct stop pair production in the allowed parameter space by performing the Monte Carlo simulations for the channel $pp \rightarrow \tilde{t}_1 \tilde{t}_1^* \rightarrow t\tilde{\chi}_1^0 \bar{t}\tilde{\chi}_1^0$ and the channel $pp \rightarrow \tilde{t}_1 \tilde{t}_1^* \rightarrow b\tilde{\chi}_1^+ \bar{b}\tilde{\chi}_1^-$. We will present their corresponding sensitivities for 8 TeV LHC and for 14 TeV LHC respectively. Finally in Sec. IV, we summarize the conclusions obtained in this work.

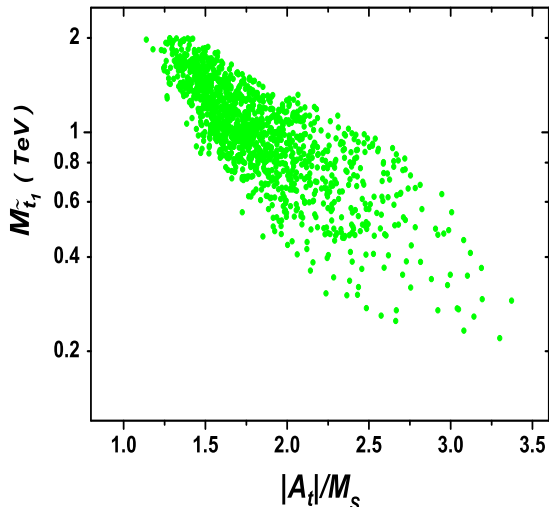


FIG. 1: Scatter plot of surviving samples in natural MSSM, projected on the plane of $m_{\tilde{t}_1}$ versus $|A_t|/M_S$. All the samples here predict the SM-like Higgs boson in the mass range 125 ± 2 GeV.

II. SCAN OVER THE PARAMETER SPACE

Motivated by the natural MSSM, we scan the parameter space of the MSSM as follows:

$$\begin{aligned}
 1 \leq \tan \beta \leq 60, \quad 100 \text{ GeV} \leq \mu \leq 200 \text{ GeV}, \quad 100 \text{ GeV} \leq M_2 \leq 1 \text{ TeV}, \\
 |A_t| \leq 3 \text{ TeV}, \quad 100 \text{ GeV} \leq (M_{\tilde{Q}_3}, M_{\tilde{U}_3}) \leq 2 \text{ TeV}, \quad 90 \text{ GeV} \leq M_A \leq 1 \text{ TeV}. \quad (4)
 \end{aligned}$$

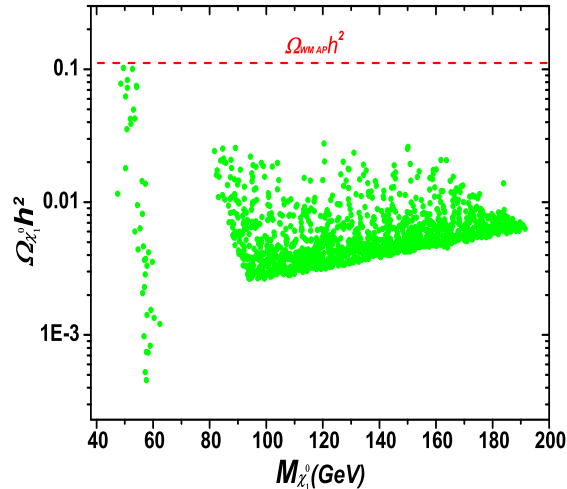


FIG. 2: Same as Fig.1, but showing the relic density of the neutralino dark matter.

For other unimportant parameters, we fix all the soft breaking parameters in the slepton sector and the first two generation sector at 10 TeV, and we assume $A_t = A_b$, $M_{\tilde{U}_3} = M_{\tilde{D}_3}$ and $M_1 : M_2 = 1 : 2$ (inspired by the grand unification relation). In our scan, we consider following constraints:

- We require the SM-like Higgs mass within the range 125 ± 2 GeV. We use the code `FeynHiggs2.8.6` [30] to calculate the mass and the code `HiggsBounds-3.8.0` [31] to consider the experimental constraints on the Higgs sector of the natural MSSM.
- Since the natural MSSM has important implications in B-physics [32], we use the code `susy_flavor v2.0` [33] to consider the constraints from the processes $B \rightarrow X_s \gamma$ and $B_{s(d)} \rightarrow \mu^+ \mu^-$.
- We consider indirect constraints from the precision electroweak observables such as ρ_t , $\sin^2 \theta_{eff}^l$, m_W and R_b . We use our own code for such calculation [34].
- We require the thermal relic density of the lightest neutralino (as the dark matter candidate) is below the WMAP value [35]. We use the code `MicrOmega v2.4` [36] to calculate the density.

After analyzing the surviving samples, we find they have two characters. One is that the Higgs mass of 125 ± 2 GeV requires $m_{\tilde{t}_1} \geq 220$ GeV and there is a rather strong correlation

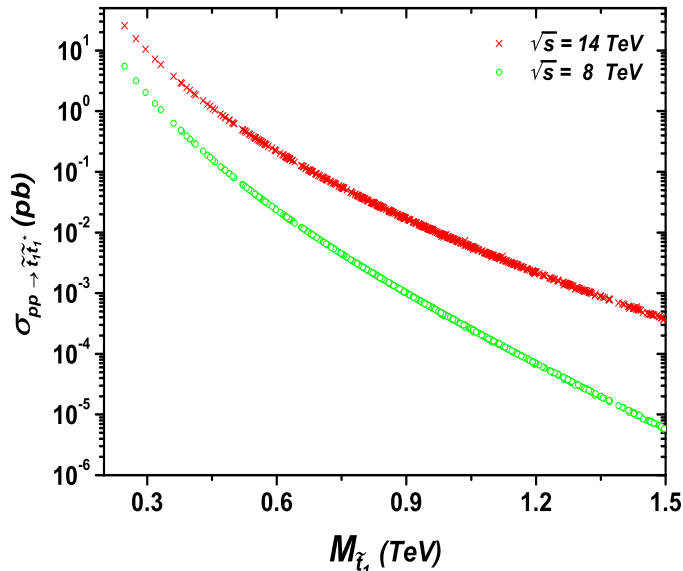


FIG. 3: Same as Fig.1, but showing the cross section of $\tilde{t}_1\tilde{t}_1^*$ production versus the stop mass.

between $m_{\tilde{t}_1}$ and the ratio $|A_t|/M_S$, as shown in Fig.1. Here we further clarify that, if $M_{\tilde{Q}_3}$ and $M_{\tilde{U}_3}$ are at sub-TeV scale, the minimum of $m_{\tilde{t}_1}$ will be enhanced to about 300 GeV [8]. The other feature is that for most cases, the values of μ are significantly smaller than M_1 so that the lightest neutralino is higgsino-like. Fig.2 indicates that the surviving samples lie within two isolated regions. We checked that the lightest neutralino is bino-like in the left region and higgsino-like in the right region. Here the bino(higgsino)-like means it is still a mixed state but the dominant component is bino(higgsino). For the light neutralino dark matter(bino-like), the main annihilation channel is through exchanging Z boson. The annihilation cross section is roughly proportional to $1/(4m_\chi^2 - m_Z^2)^2$. When the neutralino mass is about 50GeV–60GeV, the annihilation cross section may be very large, so the relic density will be less than 0.1. When the neutralino becomes heavier(60GeV–90GeV, neutralino is still bino-like), the annihilation cross section will drop. The relic density becomes large and even exceeds the WMAP value, and these samples are excluded. This is the reason for the gap between 60GeV–90GeV. When the neutralino goes on becoming heavy(>90 GeV), the dominant component of the neutralino will be higgsino. The coupling between neutralino and Higgs gets important and annihilation rate goes up, then the relic density drops.

About the natural MSSM, we have two comments. One is that in this scenario the di-photon signal of the SM-like Higgs boson can hardly be enhanced to satisfy the requirement of the LHC data. This is because in the framework of the MSSM, there are only two cases

which can enhance the di-photon rate, i.e. the small α_{eff} scenario [37, 38] and the light $\tilde{\tau}$ scenario [6, 39], and in each case a large μ is needed. In the Ref.[40], the authors pointed that the light stop with large couplings to Higgs boson in the SM+*stop* model can improve the SM fitting to the LHC and Tevatron data by enhancing $\Gamma(h \rightarrow \gamma\gamma)$ and suppressing $\Gamma(h \rightarrow gg)$. However, we should note that it does not mean that the di-photon production rate can reach the measurement of the LHC in a concrete MSSM model since the reduction of $\Gamma(h \rightarrow gg)$ is usually much stronger than the enhancement of $\Gamma(h \rightarrow \gamma\gamma)$ for large values of $X_t(X_t = A_t - \mu \tan \beta)$ [41]. The other is that recently the ATLAS collaboration searched for the gluino-mediated stop pair production followed by the decay $\tilde{t}_1 \rightarrow b\tilde{\chi}_1^+ \rightarrow b\ell\nu\tilde{\chi}_1^0$, which set a lower bound $m_{\tilde{t}_1} \geq 450$ GeV [3]. This conclusion is not applicable to the our calculations since we take the gluino mass to be larger than 1TeV in the allowed parameters space of the natural SUSY.

III. OBSERVABILITY OF STOP PAIR PRODUCTION AT THE LHC

In this section we discuss the LHC potential of discovering the stop through the direct stop pair production in the natural MSSM at $\sqrt{s} = 8, 14$ TeV. In Fig.3 we show the $pp \rightarrow \tilde{t}_1\tilde{t}_1^*$ production rate at the next leading order for the surviving samples. In getting this figure we used the package *Prospino2.1* [42] and the parton distribution function CTEQ6.6m [43] with the renormalization scale μ_R and factorization scale μ_F setting to $m_{\tilde{t}_1}$. This figure indicates that the maximal values of the cross section reach 5.5 pb and 25.7 pb for the LHC with $\sqrt{s} = 8$ TeV and $\sqrt{s} = 14$ TeV respectively, and with the increase of the stop mass, the production rates drop rapidly.

In Fig.4 we present various decay branching ratios of \tilde{t}_1 which are obtained by using the package *SDECAY* [44]. This figure indicates that for $m_{\tilde{t}_1} \leq 320$ GeV where the decay channel $\tilde{t}_1 \rightarrow t\tilde{\chi}_1^0$ does not open up, \tilde{t}_1 decays into $b\tilde{\chi}_1^+$ with a ratio of 100%, and as the stop becomes heavier, the branching ratios for $\tilde{t}_1 \rightarrow b\tilde{\chi}_1^+$ and $\tilde{t}_1 \rightarrow t\tilde{\chi}_1^0$ may still be around 50%. In contrast, the branching ratios for \tilde{t}_1 decays into $t\tilde{\chi}_{3,4}^0$ and $b\tilde{\chi}_2^+$ are usually less than 20%.

In the following we perform detailed Monte Carlo simulations to investigate the observability of the direct stop pair production at the LHC. We concentrate on the semi-leptonic analysis with the b-tagging efficiency 40%, where the signal is consisted of four jets(at least

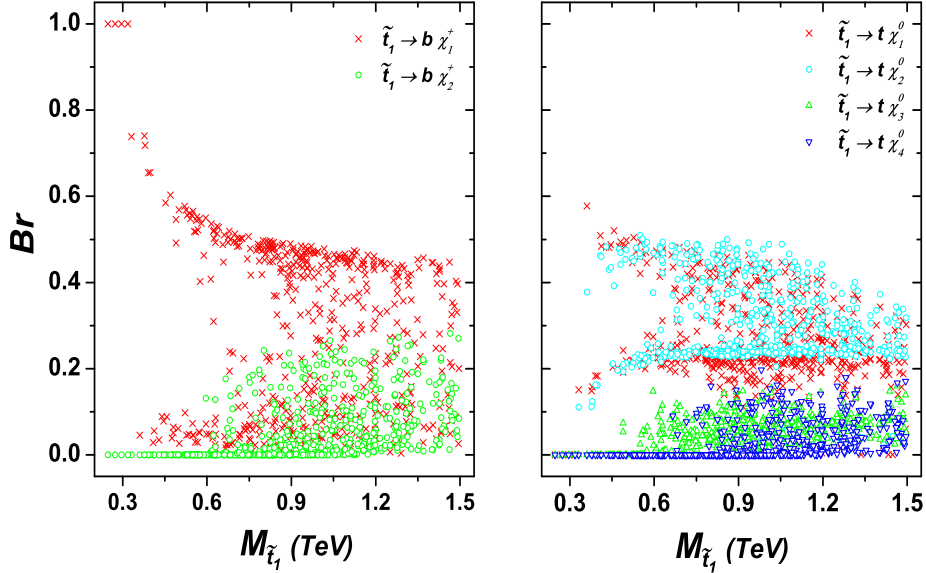


FIG. 4: Same as Fig.3, but showing the decay branching ratios of the stop.

one b-jet), one lepton (e or μ), and missing transverse energy. We first consider the process

$$pp \rightarrow \tilde{t}_1 \tilde{t}_1^* \rightarrow (t \tilde{\chi}_1^0)(\bar{t} \tilde{\chi}_1^0) \rightarrow (b \ell^+ \nu \tilde{\chi}_1^0)(\bar{b} j j \tilde{\chi}_1^0) \text{ or } (b j j \tilde{\chi}_1^0)(\bar{b} \ell^- \bar{\nu} \tilde{\chi}_1^0). \quad (5)$$

From the ATLAS search for the signal $t\bar{t} + E_T^{miss}$ [2], we can see that the dominant SM background after the E_T^{miss} and M_T cuts is $t\bar{t}$ di-leptonic channel with one lost lepton and two additional jets from initial state radiation to fake the hadronic W . Another backgrounds include $t\bar{t}$ semi-leptonic channel, $t\bar{t}$ di-leptonic channel with one τ from top decay misidentified as a jet, W +jets and $t\bar{t}Z$. Here we emphasize that the $t\bar{t}Z$ background becomes important for a heavy stop and should be considered in estimating the significance. In our calculation, we normalize the signal and the $t\bar{t}$ background to their NLO values [42, 45], and simulate the signal and backgrounds by MadGraph5 [46] interfaced with PYTHIA [47] and Delphes [48] to carry out the parton shower and fast detector simulation. We use the anti- k_t algorithm [49] with the distance parameter $R = 0.4$ to cluster jets and the MLM scheme [50] to match our matrix element with parton shower. We checked that the shapes of the matched W +1,2,3 partons are very similar, and for simplicity, we take W +2 jets samples in our calculations. In our calculations, since we employ the the variable M_{T2}^W defined in Ref.[24], we checked our results with theirs for the same parameters at $\sqrt{s} = 7$ TeV and found they were consistent with each other.

In Fig.5, we show the distributions of \cancel{E}_T , the transverse mass M_T defined in [2] and M_{T2}^W for the backgrounds and our benchmark point $m_{\tilde{t}_1} = 429$ GeV and $m_{\tilde{\chi}_1^0} = 110$ GeV

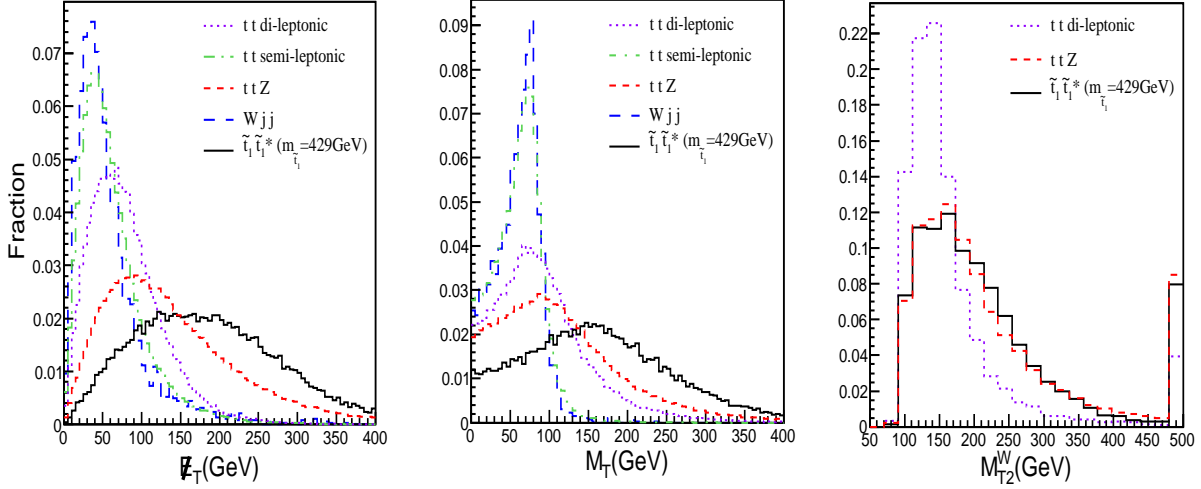


FIG. 5: The distributions of $\ell+4\text{-jets}+\cancel{E}_T$ with respect to \cancel{E}_T , M_T and M_{T2}^W for the signal $pp \rightarrow \tilde{t}_1\tilde{t}_1^* \rightarrow t\tilde{\chi}_1^0\bar{t}\tilde{\chi}_1^0$ and backgrounds. In the M_{T2}^W distribution, we impose the cuts $\cancel{E}_T > 150$ GeV and $M_T > 150$ GeV on the events and only display the di-leptonic $t\bar{t}$, $t\bar{t}Z$ backgrounds and signal, where the events with wrong or no solution for M_{T2}^W are included in the last bin.

TABLE I: The significance of stop pair production $pp \rightarrow \tilde{t}_1\tilde{t}_1^* \rightarrow t\tilde{\chi}_1^0\bar{t}\tilde{\chi}_1^0$ for 100 fb^{-1} luminosity after imposing various cuts. Here we take $m_{\tilde{t}_1} = 429$ GeV and $\tilde{\chi}_1^0 = 110$ GeV for illustration.

$\cancel{E}_T\text{-cut}$ (GeV)	$M_T\text{-cut}$ (GeV)	$M_{T2}^W\text{-cut}$ (GeV)	S/\sqrt{B} (8TeV)	S/\sqrt{B} (14TeV)
150	-	-	1.26	4.05
150	150	-	2.75	7.91
150	150	173	3.11	8.60

with $\sqrt{s} = 8$ TeV (similar results are found for $\sqrt{s} = 14$ TeV). This figure indicates that most events of $W+\text{jj}$ and semi-leptonic $t\bar{t}$ backgrounds are characterized by $\cancel{E}_T \leq 100$ GeV and $M_T \leq 100$ GeV, and most events of the di-leptonic $t\bar{t}$ backgrounds are characterized by $M_{T2}^W \leq 170$ GeV, while a significant fraction of the signal may have larger \cancel{E}_T , M_T and M_{T2}^W . Fig.5 also indicates that the distributions of the $t\bar{t}Z$ background are quite similar to the signal and are difficult to be suppressed. Fortunately, the production rate of $t\bar{t}Z$ is much smaller than the one of $\tilde{t}_1\tilde{t}_1^*$.

In Table I, we present the significance S/\sqrt{B} of our benchmark point for 100 fb^{-1} luminosity with $\sqrt{s} = 8$ TeV and 14 TeV respectively by sequentially imposing the cuts on \cancel{E}_T , M_T and M_{T2}^W . It can be seen that, for the given reference point, the cut $M_T > 150$ GeV can

greatly enhance the significance and $M_{T2}^W > 173$ GeV further improves the significance by about 14% for $\sqrt{s} = 8$ TeV and 9% for $\sqrt{s} = 14$ TeV to reach 3.11 and 8.60 respectively.

Therefore, for our simulations in the allowed parameters space, we take the following events selection criteria:

- One isolated electron or muon that passes the following requirements;
 - Electrons $E_T > 25\text{GeV}$ and $|\eta| < 2.47$ without $1.37 < |\eta| < 1.52$;
 - Muon: $E_T > 20\text{GeV}$ and $|\eta| < 2.5$;
 - Events are rejected if they contain a second lepton candidate with $P_T > 15\text{GeV}$;
- Four or more reconstructed jets with $P_T > 25\text{GeV}$ and $|\eta| < 2.5$.
- $\cancel{E}_T > 150\text{GeV}$, $M_T > 150\text{GeV}$, $M_{T2}^W > 173\text{GeV}$.

where the basic cuts about p_T and η on leptons and jets are from the ATLAS report[2]. In order to improve the signal sensitivity, we increase the values of ATLAS cut \cancel{E}_T from 100 GeV to 150 GeV to further suppress the semi-leptonic $t\bar{t}$ background and use the new cut $M_{T2}^W > 173$ GeV to reduce the di-leptonic $t\bar{t}$ background in our calculations.

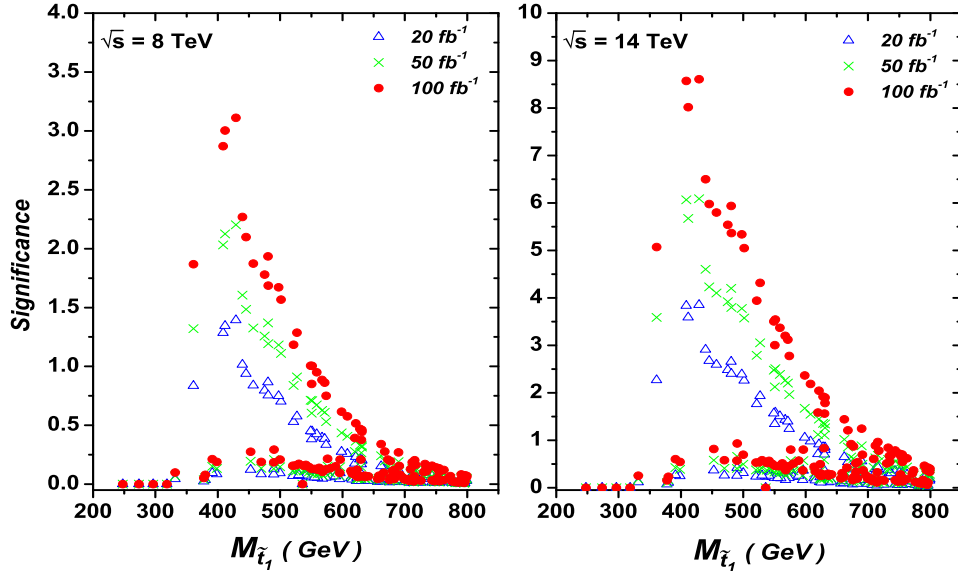


FIG. 6: The significance of stop pair production $pp \rightarrow \tilde{t}_1 \tilde{t}_1^* \rightarrow t \tilde{\chi}_1^0 \bar{t} \tilde{\chi}_1^0$ for the surviving samples in the natural MSSM.

In Fig.6 we show the significance of the surviving samples with $m_{\tilde{t}_1} < 800$ GeV. This figure indicates that the largest significance can be reached at $m_{\tilde{t}_1} \simeq 430$ GeV where the

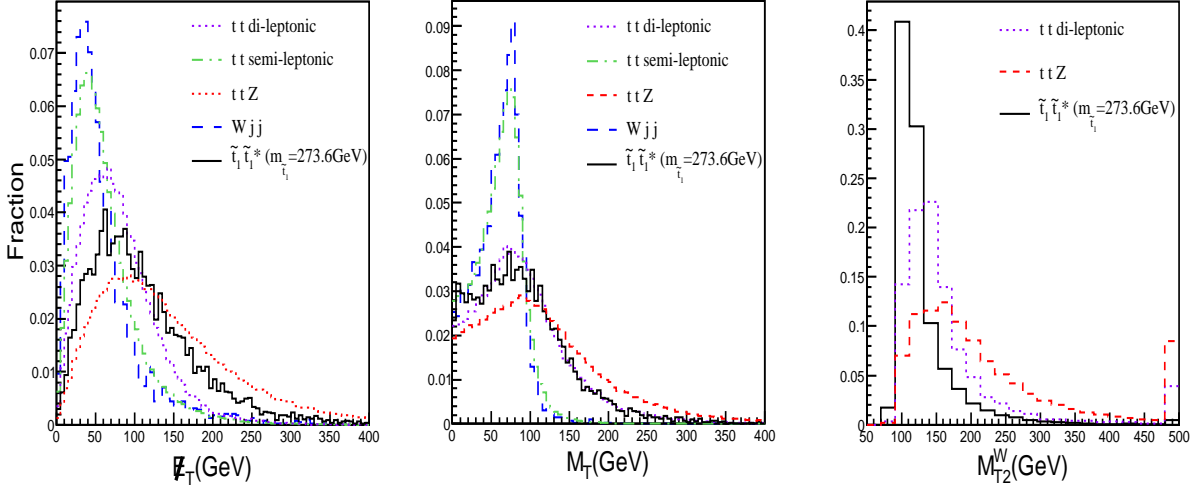


FIG. 7: Same as Fig.5, except that in plotting M_{T2}^W distribution we impose the cuts $\cancel{E}_T > 100$ GeV and $M_T > 100$ GeV on the events.

significance is about 1.5 for $\sqrt{s} = 8$ TeV with $20 fb^{-1}$ luminosity and 8.5 for $\sqrt{s} = 14$ TeV with $100 fb^{-1}$ luminosity, and with the increase of the stop mass, the significance drop by one half for $m_{\tilde{t}_1} \simeq 500$ GeV mainly due to the reduction of the production rate. Our results are not as optimistic as those in [20, 21, 24] because we have taken into account the branch ratio of $\tilde{t}_1 \rightarrow t\tilde{\chi}_1^0$. Fig.6 also indicates that there are two branches for the significance in the mass region $320 \text{ GeV} < m_{\tilde{t}_1} < 600 \text{ GeV}$. We checked that the upper branch corresponds to high branching ratio of $\tilde{t}_1 \rightarrow t\tilde{\chi}_1^0$, which varies from 42.1% to 57.7% and results in a large signal rate, while the lower branch corresponds to a small ratio due to the competition of the decay mode $\tilde{t}_1 \rightarrow t\tilde{\chi}_1^0$ with $\tilde{t}_1 \rightarrow b\tilde{\chi}_1^+$ and $\tilde{t}_1 \rightarrow t\tilde{\chi}_2^0$.

Above analysis implies that, in order to fully explore the parameter space of the natural MSSM in stop detection, the decay mode $\tilde{t}_1 \rightarrow b\tilde{\chi}_1^+$ should also be considered. So we next consider the process

$$pp \rightarrow \tilde{t}_1 \tilde{t}_1^* \rightarrow (b\tilde{\chi}_1^+)(\bar{b}\tilde{\chi}_1^-) \rightarrow (b\ell^+ \nu \tilde{\chi}_1^0)(\bar{b}jj\tilde{\chi}_1^0) \text{ or } (bjj\tilde{\chi}_1^0)(\bar{b}\ell^- \bar{\nu}\tilde{\chi}_1^0). \quad (6)$$

Same as in Fig.5, we show the distributions of the three variables in Fig.7 for the benchmark point $m_{\tilde{t}_1} = 273.6$ GeV, $m_{\tilde{\chi}_1^+} = 163.5$ GeV and $m_{\tilde{\chi}_1^0} = 156.3$ GeV. Compared with the distribution in Fig.5, one can see that more signal events have lower values of \cancel{E}_T and low M_T , due to the relatively light \tilde{t}_1 . Fig.7 also indicates the M_{T2}^W variable is helpless in suppressing the di-leptonic $t\bar{t}$ events and any cut on M_{T2}^W may hurt the signal greatly.

In Fig.8, we show the significance of the surviving samples for the process in Eq.(6). In

order to keep more signal events, here we relax the cuts of \cancel{E}_T and M_T used for the process in Eq.(5) as follows:

$$\cancel{E}_T > 100 \text{ GeV}, \quad M_T > 100 \text{ GeV}. \quad (7)$$

From this figure, one can learn that, due to the large stop pair production rate, the significance for $m_{\tilde{t}_1} = 250 \text{ GeV}$ may reach 7 for $\sqrt{s} = 8 \text{ TeV}$ with 20 fb^{-1} luminosity and 64 for $\sqrt{s} = 14 \text{ TeV}$ with 100 fb^{-1} luminosity, but for $m_{\tilde{t}_1} = 400 \text{ GeV}$, the maximum value drops to 1.5 and 10 respectively.

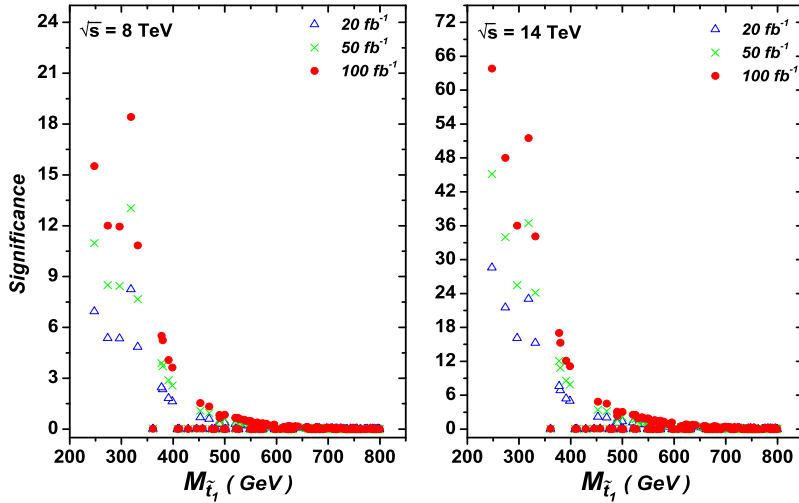


FIG. 8: The significance of stop pair production $pp \rightarrow \tilde{t}_1 \tilde{t}_1^* \rightarrow (b\tilde{\chi}_1^+)(\bar{b}\tilde{\chi}_1^-)$ for the surviving samples in the natural MSSM.

Finally, we summary the significance of the direct stop pair production with the above two decay modes of \tilde{t}_1 for $\sqrt{s} = 14 \text{ GeV}$ and 100 fb^{-1} luminosity. The results are displayed in Fig.9 where only the maximal significance under each cut is shown. This figure indicates that, for $m_{\tilde{t}_1} < 400 \text{ GeV}$, detecting the stop pair production through the chargino decay is more effective, while for $400 \text{ GeV} \leq m_{\tilde{t}_1} \leq 450 \text{ GeV}$ the neutralino decay is more effective. This figure also indicates that the LHC can discover \tilde{t}_1 predicated in nature MSSM up to 450 GeV . If no excess events were observed at the LHC, the 95% C.L. exclusion limits of the stop masses can go up to around 537 GeV no matter what decay modes of the stop in the natural MSSM.

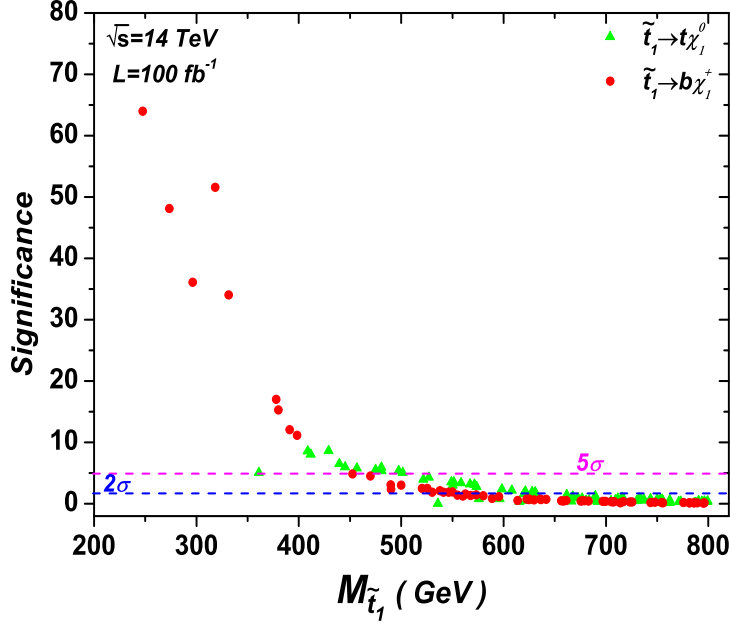


FIG. 9: The maximal significance in Eq.(5) or Eq.(6) as a function of the stop mass. The bullets (red) are obtained in Eq.(6) while the triangles (green) are obtained in Eq.(5).

IV. CONCLUSION

In this work we studied the direct stop pair production at the LHC in the natural MSSM. We scanned over the corresponding parameter space by considering various experimental constraints and then in the allowed parameter space we examined the observability of the direct stop pair production at the LHC through the semi-leptonic analysis. We focused on the following two channels

$$\begin{aligned}
 pp &\rightarrow \tilde{t}_1\tilde{t}_1^* \rightarrow (t\tilde{\chi}_1^0)(\bar{t}\tilde{\chi}_1^0) \rightarrow (b\ell^+\nu\tilde{\chi}_1^0)(\bar{b}j\tilde{\chi}_1^0) \text{ or } (bjj\tilde{\chi}_1^0)(\bar{b}\ell^-\bar{\nu}\tilde{\chi}_1^0), \\
 pp &\rightarrow \tilde{t}_1\tilde{t}_1^* \rightarrow (b\tilde{\chi}_1^+)(\bar{b}\tilde{\chi}_1^-) \rightarrow (b\ell^+\nu\tilde{\chi}_1^0)(\bar{b}j\tilde{\chi}_1^0) \text{ or } (bjj\tilde{\chi}_1^0)(\bar{b}\ell^-\bar{\nu}\tilde{\chi}_1^0),
 \end{aligned}$$

and performed detailed Monte Carlo simulations about the signals and backgrounds. We found that for $m_{\tilde{t}_1} < 400\text{GeV}$ the second channel is better while for $400\text{GeV} \leq m_{\tilde{t}_1} \leq 450\text{GeV}$ the first channel is better. We also found that the LHC with $\sqrt{s} = 14\text{TeV}$ and 100fb^{-1} luminosity is capable of discovering \tilde{t}_1 predicted in nature MSSM up to 450GeV. If no excess events were observed at the LHC, the 95% C.L. exclusion limits of the stop masses can reach around 537 GeV in the natural MSSM.

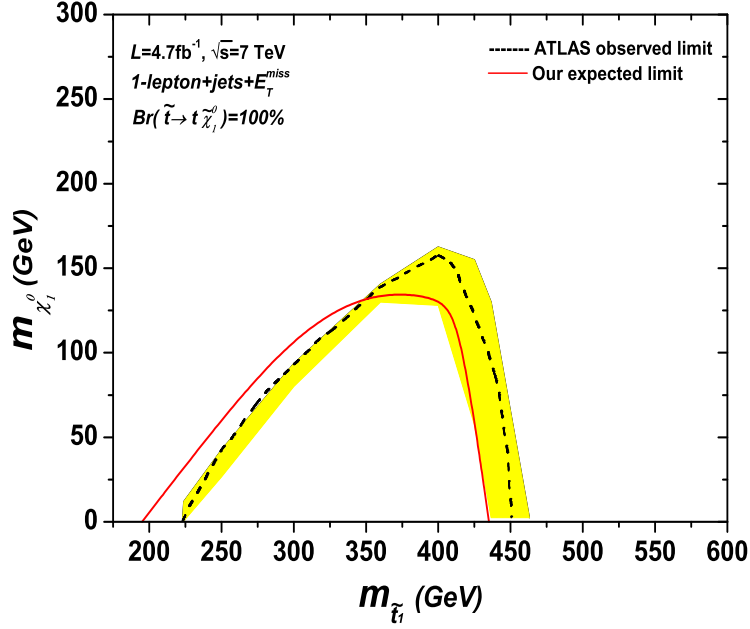


FIG. 10: The ATLAS observed and our expected exclusion limit in the plane of $m_{\tilde{\chi}_1^0}$ versus $m_{\tilde{t}_1}$, assuming $BR(\tilde{t}_1 \rightarrow t\tilde{\chi}_1^0) = 100\%$.

Note Added

Very recently, the ATLAS collaboration reported the result of the direct searching for the stop pair production base on $4.7fb^{-1}$ of data[51]. We validated our simulation by reproducing the ATLAS exclusion limit according to the assumptions and cuts in the report as follows:

- One isolated electron or muon passing ‘tight’ selection criteria;
 - Electrons $E_T > 25\text{GeV}$ and $|\eta| < 2.47$;
 - Muon: $E_T > 20\text{GeV}$ and $|\eta| < 2.4$.
- Four or more jets with $|\eta| < 2.5$ and $P_T > 80, 60, 40$ and 25 GeV, and at least one jet to be identified as a b-jet;
- $\Delta\phi_{min} > 0.8$, where $\Delta\phi_{min}$ is the minimum azimuthal separation between the two highest P_T jets and the missing transverse momentum direction;

- The jet-jet pair having invariant mass > 60 GeV and the smallest ΔR is selected to form the hadronically decaying W boson. The mass m_{jjj} is reconstructed including a third jet closest in ΔR to the hadronic W boson momentum vector and $130 \text{ GeV} < m_{jjj} < 205 \text{ GeV}$ is required;
- $E_T^{miss} > 150 \text{ GeV}$, $E_T^{miss}/\sqrt{H_T} > 7 \text{ GeV}^{1/2}$ and $m_T > 120 \text{ GeV}$;
- Events are rejected if they contain additional leptons passing looser selection criteria. Here we treat the looser selection criteria as $P_T > 15 \text{ GeV}$.
- The branch ratio of $\tilde{t}_1 \rightarrow t\tilde{\chi}_1^0$ is assumed to be 100%.

In Fig.10, we display the expected exclusion limit from our simulation. Considering the differences between the fast simulation and full detector simulation, we can see that our result is consistent with the ATLAS exclusion limit within the reasonable error range. We also expect our result can be improved by the simultaneous fits method used by ATLAS for five signal regions and three control regions, however, which is beyond the scope of our simulation. It should be noted that the above stop masses limits can be avoided in our study, since the stop decays with a mixture of the branching ratios.

Acknowledgement

Lei Wu thanks Xerxes Tata, Zijun Xu and Qiang Li for helpful discussion about the natural SUSY and MG/ME, and appreciates the organizers and lecturers at the KIAS school on MadGraph for LHC physics simulation (Oct. 24-29, 2011, KIAS, Seoul). This work was supported in part by the National Natural Science Foundation of China (NNSFC) under grant Nos. 10821504, 11135003, 10775039, 11075045, by Specialized Research Fund for the Doctoral Program of Higher Education with grant No. 20104104110001, and by the Project of Knowledge Innovation Program (PKIP) of Chinese Academy of Sciences under grant No. KJCX2.YW.W10.

[1] ATLAS Collaboration, ATLAS-CONF-2012-093; CMS Collaboration, CMS-PAS-HIG-12-020; G. Aad *et al.* [ATLAS Collaboration], Phys. Lett. B **710**, 49 (2012); S. Chatrchyan *et al.*

- [CMS Collaboration], Phys. Lett. B **710**, 26 (2012).
- [2] G. Aad *et al.* [ATLAS Collaboration], Phys. Rev. Lett. **108**, 041805 (2012).
- [3] G. Aad *et al.* [ATLAS Collaboration], Phys. Rev. D **85**, 112006 (2012); Phys. Rev. Lett. **108**, 241802 (2012); Phys. Rev. Lett. **108**, 181802 (2012).
- [4] V. M. Abazov *et al.* [D0 Collaboration], Phys. Lett. B **710**, 578 (2012); Phys. Lett. B **696**, 321 (2011); T. Aaltonen *et al.* [CDF Collaboration], Phys. Rev. Lett. **106**, 191801 (2011); Phys. Rev. Lett. **107**, 191803 (2011).
- [5] S. Chatrchyan *et al.* [CMS collaboration], Phys. Rev. Lett. **107**, 221804 (2011); G. Aad *et al.* [ATLAS collaboration], arXiv:1109.6572 [hep-exp].
- [6] M. Carena, S. Gori, N. R. Shah and C. E. M. Wagner, JHEP **1203**, 014 (2012).
- [7] see, e.g., J. Cao *et al.* Phys. Lett. B **710**, 665 (2012); H. Baer, V. Barger and A. Mustafayev, JHEP **1205**, 091 (2012); L. Aparicio, D. G. Cerdeno and L. E. Ibanez, JHEP **1204**, 126 (2012); J. Ellis, K. A. Olive and K. A. Olive, Eur. Phys. J. C **72**, 2005 (2012); C. Balazs *et al.*, arXiv:1205.1568. A. Fowlie *et al.*, arXiv:1206.0264;
- [8] J. Cao, *et al.*, JHEP **1203**, 086 (2012).
- [9] see, e.g., U. Ellwanger, JHEP **1203**, 044 (2012); J. F. Gunion, Y. Jiang and S. Kraml, Phys. Lett. B **710**, 454 (2012); U. Ellwanger and C. Hugonie, arXiv:1203.5048 [hep-ph]; D. A. Vasquez *et al.*, Phys. Rev. D **86**, 035023 (2012).
- [10] R. Arnowitt and P. Nath, Phys. Rev. D **46**, 3981 (1992).
- [11] S. F. King, M. Muhlleitner and R. Nevzorov, Nucl. Phys. B **860**, 207 (2012).
- [12] P. Huet and A. E. Nelson, Phys. Rev. D **53** (1996) 4578; M. Carena, G. Nardini, M. Quiros and C. E. M. Wagner, Nucl. Phys. B **812** (2009) 243; Y. Li, S. Profumo and M. Ramsey-Musolf, Phys. Lett. B **673** (2009) 95.
- [13] K. Griest and D. Seckel, Phys. Rev. D **43** (1991) 3191; C. Boehm, A. Djouadi and M. Drees, Phys. Rev. **D62** (2000) 035012.
- [14] C. Brust, A. Katz, S. Lawrence and R. Sundrum, JHEP **1203**, 103 (2012).
- [15] D. Feldman, G. Kane, E. Kuflik and R. Lu, Phys. Lett. B **704**, 56 (2011); H. Baer *et al.*, JHEP **1010**, 018 (2010); A. Cohen, D. B. Kaplan and A. Nelson, Phys. Lett. B **388**, 588 (1996); M. Dine, A. Kagan and S. Samuel, Phys. Lett. B **243**, 250 (1990).
- [16] J. L. Feng and D. Sanford, arXiv:1205.2372 [hep-ph]; G. Bhattacharyya and T. S. Ray, JHEP **1205**, 022 (2012); S. Krippendorff, H. P. Nilles, M. Ratz and M. W. Winkler, Phys. Lett. B

- 712**, 87 (2012); B. C. Allanach and B. Gripaios, *JHEP* **1205**, 062 (2012); S. Akula, M. Liu, P. Nath and G. Peim, *Phys. Lett. B* **709**, 192 (2012); L. J. Hall, D. Pinner and J. T. Ruderman, *JHEP* **1204**, 131 (2012); M. Asano, H. D. Kim, R. Kitano and Y. Shimizu, *JHEP* **1012**, 019 (2010); R. Kitano and Y. Nomura, *Phys. Rev. D* **73**, 095004 (2006); J. Hisano, K. Kurosawa and Y. Nomura, *Nucl. Phys. B* **584**, 3 (2000); J. L. Feng, K. T. Matchev and T. Moroi, *Phys. Rev. D* **61**, 075005 (2000); K. L. Chan, U. Chattopadhyay and P. Nath, *Phys. Rev. D* **58**, 096004 (1998); G. W. Anderson, D. J. Castano and A. Riotto, *Phys. Rev. D* **55**, 2950 (1997).
- [17] H. Baer, V. Barger, P. Huang and X. Tata, *JHEP* **1205**, 109 (2012).
- [18] M. Papucci, J. T. Ruderman and A. Weiler, arXiv:1110.6926 [hep-ph];
- [19] see, e.g., A. Choudhury and A. Datta, *JHEP* **1206**, 006 (2012)? K. Huitu, L. Leinonen and J. Laamanen, *Phys. Rev. D* **84**, 075021 (2011); Y. Kats and D. Shih, *JHEP* **1108**, 049 (2011); S. Bornhauser, M. Drees, S. Grab and J. S. Kim, *Phys. Rev. D* **83**, 035008 (2011); N. Bhattacharyya, A. Choudhury and A. Datta, *Phys. Rev. D* **84**, 095006 (2011); D. Casadei, R. Konoplich and R. Djilkibaev, *Phys. Rev. D* **82**, 075011 (2010); K. Rolbiecki, J. Tattersall and G. Moortgat-Pick, *Eur. Phys. J. C* **71**, 1517 (2011); M. Perelstein and A. Weiler, *JHEP* **0903**, 141 (2009); T. Han, R. Mahbubani, D. G. E. Walker and L. -T. Wang, *JHEP* **0905**, 117 (2009); M. Carena, A. Freitas and C. E. M. Wagner, *JHEP* **0810**, 109 (2008); S. Kraml and A. R. Raklev, *Phys. Rev. D* **73**, 075002 (2006); T. Han et al., *Phys. Rev. D* **70**, 055001 (2004). A. Bartl et al., *Phys. Lett. B* **573**, 153 (2003); J. Hisano, K. Kawagoe and M. M. Nojiri, *Phys. Rev. D* **68**, 035007 (2003); J. Hisano, K. Kawagoe, R. Kitano and M. M. Nojiri, *Phys. Rev. D* **66**, 115004 (2002); J. M. Yang and B. -L. Young, *Phys. Rev. D* **62**, 115002 (2000);
- [20] D. E. Kaplan, K. Rehermann and D. Stolarski, *JHEP* **1207**, 119 (2012).
- [21] T. Plehn, M. Spannowsky and M. Takeuchi, *JHEP* **1208**, 091 (2012); *Phys. Rev. D* **85**, 034029 (2012); *JHEP* **1105**, 135 (2011); T. Plehn and M. Spannowsky, arXiv:1112.4441; T. Plehn et al., *JHEP* **1010**, 078 (2010); T. Plehn, G. P. Salam and M. Spannowsky, *Phys. Rev. Lett.* **104**, 111801 (2010).
- [22] J. Thaler and K. Van Tilburg, *JHEP* **1202**, 093 (2012); J. Thaler and K. Van Tilburg, *JHEP* **1103**, 015 (2011); J. Thaler and L. -T. Wang, *JHEP* **0807**, 092 (2008).
- [23] K. Rehermann and B. Tweedie, *JHEP* **1103**, 059 (2011); M. Jankowiak and A. J. Larkoski, *JHEP* **1106**, 057 (2011); L. G. Almeida et al., *Phys. Rev. D* **82**, 054034 (2010); *Phys. Rev. D* **79**, 074012 (2009); D. E. Kaplan et al., *Phys. Rev. Lett.* **101**, 142001 (2008).

- [24] Y. Bai, H. -C. Cheng, J. Gallicchio and J. Gu, arXiv:1203.4813 [hep-ph].
- [25] Z. Han, A. Katz, D. Krohn and M. Reece, JHEP **1208**, 083 (2012).
- [26] M. Drees, M. Hanussek and J. S. Kim, arXiv:1201.5714 [hep-ph];
- [27] D. S. M. Alves et al., arXiv:1205.5805 [hep-ph];
- [28] C. Brust, A. Katz and R. Sundrum, JHEP **1208**, 059 (2012); H. -T. Wei, et al., JHEP **1107**, 003 (2011); N. Desai and B. Mukhopadhyaya, JHEP **1010**, 060 (2010).
- [29] X. -J. Bi, Q. -S. Yan and P. -F. Yin, Phys. Rev. D **85**, 035005 (2012);
- [30] M. Frank et al., JHEP **0702**, 047 (2007); G. Degrassi et al., Eur. Phys. J. C **28**, 133 (2003); S. Heinemeyer, W. Hollik and G. Weiglein, Comput. Phys. Commun. **124**, 76 (2000); Eur. Phys. J. C **9**, 343 (1999).
- [31] P. Bechtle et al., Comput. Phys. Commun. **182**, 2605 (2011); Comput. Phys. Commun. **181**, 138 (2010).
- [32] K. Ishiwata, N. Nagata and N. Yokozaki, Phys. Lett. B **710**, 145 (2012).
- [33] J. Rosiek et al., Comput. Phys. Commun. **181**, 2180 (2010); A. Crivellin, L. Hofer and J. Rosiek, JHEP **1107**, 017 (2011).
- [34] J. Cao and J. M. Yang, JHEP **0812**, 006 (2008).
- [35] J. Dunkley *et al.* [WMAP Collaboration], Astrophys. J. Suppl. **180**, 306 (2009)
- [36] G. Belanger et al., Comput. Phys. Commun. **182**, 842 (2011).
- [37] M. S. Carena et al., Eur. Phys. J. C **26**, 601 (2003).
- [38] J. Cao et al., Phys. Lett. B **703**, 462 (2011);
- [39] M. Carena et al., arXiv:1205.5842 [hep-ph].
- [40] M. R. Buckley and D. Hooper, arXiv:1207.1445 [hep-ph].
- [41] A. Djouadi, Phys. Lett. B **435**, 101 (1998); [hep-ph/9901237].
- [42] W. Beenakker et al., Nucl. Phys. B **515**, 3 (1998);
- [43] J. Pumplin *et al.*, JHEP **0602**, 032 (2006).
- [44] M. Muhlleitner, A. Djouadi and Y. Mambrini, Comput. Phys. Commun. **168**, 46 (2005).
- [45] N. Kidonakis, Phys. Rev. D **82**, 114030 (2010); V. Ahrens et al., Phys. Lett. B **703**, 135 (2011); M. Cacciari et al., Phys. Lett. B **710**, 612 (2012); S. Moch, P. Uwer and A. Vogt, arXiv:1203.6282.
- [46] J. Alwall et al., JHEP **1106**, 128 (2011).
- [47] T. Sjostrand, S. Mrenna and P. Z. Skands, JHEP **0605**, 026 (2006).

- [48] S. Oryn, X. Rouby and V. Lemaitre, arXiv:0903.2225 [hep-ph].
- [49] M. Cacciari, G. P. Salam and G. Soyez, JHEP **0804**, 063 (2008).
- [50] F. Caravaglios, M. L. Mangano, M. Moretti and R. Pittau, Nucl. Phys. B **539**, 215 (1999).
- [51] G. Aad *et al.* [ATLAS Collaboration], arXiv:1208.2590 [hep-ex].